AIP | Applied Physics Letters

Asymmetric hysteresis loops and its dependence on magnetic anisotropy in exchange biased Co/CoO core-shell nanoparticles

Sayan Chandra, Hafsa Khurshid, Manh-Huong Phan, and Hariharan Srikanth

Citation: Appl. Phys. Lett. **101**, 232405 (2012); doi: 10.1063/1.4769350
View online: http://dx.doi.org/10.1063/1.4769350
View Table of Contents: http://apl.aip.org/resource/1/APPLAB/v101/i23
Published by the American Institute of Physics.

Related Articles

Defect mediated reversible ferromagnetism in Co and Mn doped zinc oxide epitaxial films
J. Appl. Phys. 112, 113917 (2012)

Spacer-less, decoupled granular L10 FePt magnetic media using Ar–He sputtering gas
J. Appl. Phys. 112, 113916 (2012)

Magnetic moment manipulation by triplet Josephson current
Appl. Phys. Lett. 101, 242602 (2012)

An improved magnetic field detection unit based on length-magnetized Terfenol-D and width-polarized ternary 0.35Pb(In1/2Nb1/2)O3-0.35Pb(Mg1/3Nb2/3)O3-0.30PbTiO3
Appl. Phys. Lett. 101, 232906 (2012)

Exchange bias effect in CoFe2O4-Cr2O3 nanocomposite embedded in SiO2 matrix
J. Appl. Phys. 112, 113905 (2012)

Additional information on Appl. Phys. Lett.

Journal Homepage: http://apl.aip.org/
Journal Information: http://apl.aip.org/about/about_the_journal
Top downloads: http://apl.aip.org/features/most_downloaded
Information for Authors: http://apl.aip.org/authors

ADVERTISEMENT

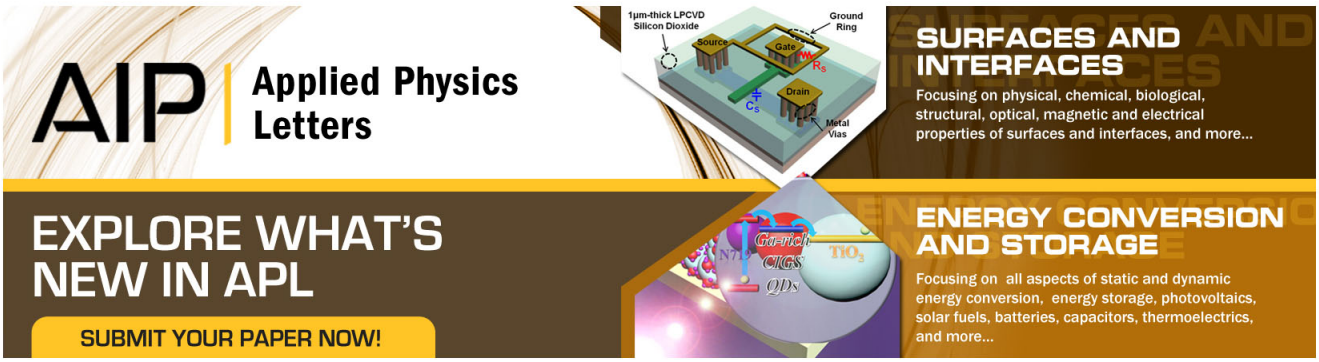

Asymmetric hysteresis loops and its dependence on magnetic anisotropy in exchange biased Co/CoO core-shell nanoparticles

Sayan Chandra, Hafsa Khurshid, Manh-Huong Phan, and Hariharan Srikanth[a)]
Department of Physics, University of South Florida, Tampa, Florida 33620, USA

(Received 5 September 2012; accepted 15 November 2012; published online 4 December 2012)

The origin of asymmetry in field cooled (FC) hysteresis loops exhibiting exchange bias (EB) is investigated by studying the static and dynamic magnetic properties of core-shell Co/CoO nanoparticles. Two distinct freezing temperatures coresponding to the core ($T_{f\text{-}cr} \sim 190$ K) and the shell moments ($T_{f\text{-}sh} \sim 95$ K) are obtained from the energy barrier distribution. The FC loops are symmetric in the temperature range $T_{f\text{-}sh} \leq T \leq T_{f\text{-}cr}$, however, asymmetry in hysteresis is observed immediately below $T_{f\text{-}sh}$. These intriguing features are also probed by radio frequency transverse susceptibility (TS) experiments. We show that the first anisotropy fields obtained from the demagnetization and return curves of field cooled TS measurement, shift along the negative field axis and strikingly resemble the temperature dependence of EB. Field cooled TS measurements reveal the effect of competing Zeeman and anisotropy energy above and below $T_{f\text{-}sh}$ to account for the development of asymmetry. Our study indicates that asymmetry in FC hysteresis loops is intrinsic to core-shell nanoparticles and develops only below the freezing temperature of the shell due to enhanced magnetic anisotropy. © *2012 American Institute of Physics*.
[http://dx.doi.org/10.1063/1.4769350]

Exchange bias (EB) has been an intense area of research from both fundamental and application point of view.[1–3] In case of core-shell nanoparticles, EB has been observed in ferromagnetic (FM) core/antiferromagnetic (AFM) shell,[4,5] FM core/ferrimagnetic (FIM) shell,[6] and more recently in AFM core/FIM shell.[7] The role of disordered surface spins in case of ferrites and interfacial spins within the core-shell arrangement have been studied and are essential in understanding EB.[8,9] A common feature in a field-cooled (FC) hysteresis loop for a system exhibiting EB is vertical shift along the magnetization axis and asymmetry in the magnetization lobes.[10] The vertical shift in FC loops is attributed to uncompensated spins.[9,11] Monte Carlo simulations have shown that the net magnetization of the spins at the shell interface is responsible for the asymmetry.[12,13] Despite this, there are reports of nanoparticles with core-shell morphology that exhibit EB without or negligible asymmetry in the hysteresis loops.[14,15] Although a lot of research has been carried out for exchange biased multilayer thin films to understand the origin of asymmetry,[16] there are few experimental studies in case of core-shell nanoparticles. An important question emerges: Is it possible to deliberately introduce and tune asymmetry in magnetic hysteresis of nanoparticles exhibiting exchange bias? If true, then how does the magnetic anisotropy of the nanoparticles alter with the development of asymmetry? It has been reported that the "shell" plays an essential role in stabilizing magnetism of core-shell nanoparticles and has been proposed to be crucial for applicability of future recording media.[17]

In this letter, we have demonstrated that the magnetic state of the "shell" holds the key to the presence or the absence of asymmetry in FC hysteresis loops. The system under study is ~19 nm Co/CoO nanoparticles. We have experimentally distinguished the individual temperature dependent magnetic response of the core and shell. This gives us information about the instantaneous magnetic state of the core and shell as asymmetry develops. In addition, our transverse susceptibility (TS) measurements provide a direct estimate of the magnetic anisotropy and its evolution with temperature as asymmetry sets in. Our analysis can be extended to core-shell nanoparticles with different compositions and suggests that it may be possible to selectively choose the material constituting the shell to gain control over the onset of asymmetry in a desired temperature range. We believe that knowledge about the presence or the absence of asymmetry in hysteresis loops may be used to advantage while designing future applications based on exchange bias.

The core-shell structured nanoparticles were synthesized by high temperature reduction of di-cobalt-octa-carbonyl in octadecene in the presence of olyelamine (OY) and oleic acid (OA). The synthesis route adopted is modified from the previous reaction route reported.[18] Fig. 1(a) shows a conventional bright field transmission electron microscope (TEM) image of the as synthesized nanoparticles. In the selected area diffraction pattern [Fig. 1(b)], well defined rings corresponding to the Co core and the CoO shell are seen which suggest that the core and the shell are highly crystalline without the presence of any amorphous phase. The high resolution transmission electron microscope (HRTEM) image [Fig. 1(c)] further reveals that the core is single crystalline with spacing corresponding to the (101) planes of hcp cobalt whereas the shell is composed of randomly oriented small crystallites. A representative histogram of the particle size distribution is shown in Fig. 1(d). The mean particle size is determined to be 19.3 ± 3.1 nm.

The dc magnetic properties of the core-shell nanoparticles were measured using a quantum design physical properties measurement system (PPMS) with a vibrating sample magnetometer (VSM) option. Fig. 2 shows the temperature dependence of magnetization in the temperature range of 5 K to 345 K measured under an applied field of 100 Oe following the zero

[a)]Author to whom correspondence should be addressed. Electronic mail: sharihar@usf.edu.

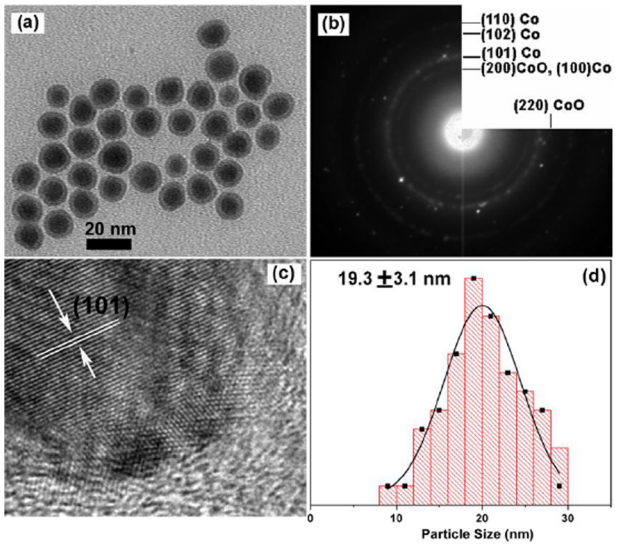

FIG. 1. (a) Bright TEM image, (b) selected area diffraction pattern, (c) HRTEM image, and (d) histogram representing particle size distribution of core-shell Co-CoO nanoparticles.

field cool (ZFC) and FC protocols. It can be seen that the ZFC and FC curves show irreversibility up to 345 K which indicates that the nanoparticles have a blocking temperature $T_B > 345$ K. Magnetization in the ZFC curve (M_{ZFC}) decreases steadily as the temperature is lowered. A distinct change in slope is observed in M_{ZFC} at ~100 K below which the rate of change in M_{ZFC} decreases. In the inset, a magnified image of the FC curve is shown. The FC magnetization (M_{FC}) shows a peak at the Neel temperature ($T_N \sim 235$ K) of the antiferromagnetic CoO shell which is consistent with earlier reports.[5] As the temperature is further lowered below T_N, the M_{FC} decreases at first followed by an increase below $T_1 \sim 95$ K. This kind of behavior in M_{FC} has been reported earlier in super spin glass (SSG) systems,[6] or in nanoparticles that undergo surface spin freezing along the direction of the cooling field.[19] A distinct change in slope of M_{ZFC} along with an increase in M_{FC} below T_1 hints to a change in the magnetic state of the sample.

We performed exchange bias experiments on the Co-CoO nanoparticles by measuring hysteresis loops in the ZFC and FC (1 T) protocol. In the insets of Fig. 3(a), M(H) loops

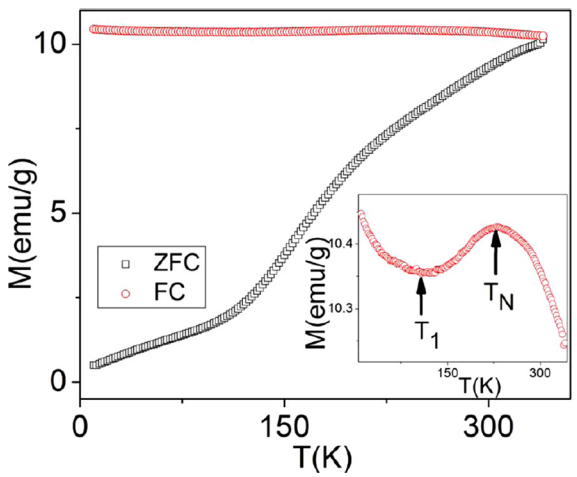

FIG. 2. Magnetization vs. temperature curve in ZFC and FC protocols. Inset shows a magnified image of the FC curve.

at 10 K and 100 K are shown for both the ZFC and FC conditions. A clear shift of the FC loop along the negative field axis confirms EB in the nanoparticle system. The EB field is calculated as $H_{EB}\left[=\frac{|(H^+ + H^-)|}{2}\right]$, where H^+ and H^- are the coercive fields for the ascending and descending curves, respectively. The temperature dependence of H_{EB} is shown in Fig. 3(a). Exchange bias develops below ~190 K; however, a significant increase in H_{EB} is seen only below $T_2 \sim 160$ K. In order to interpret this behavior, it is important to get insights into the magnetic state of the core and the shell separately. Recent reports have suggested that below T_N, as the temperature is decreased, EB develops from the blocking temperature of the Co core.[4] It has also been seen that EB may not be distinct if the individual grains constituting the AFM CoO shell behave superparamagnetically below T_N.[20] It is known that any blocking or freezing phenomenon in an ensemble of nanoparticles is associated with a change in the energy barrier distribution.[21] So, it becomes imperative in the case of our Co-CoO nanoparticles to map out the energy barrier distribution with respect to temperature, which in turn will allow us to identify any magnetic transition or crossover present in the sample. A useful method to estimate the energy barrier distribution is from temperature decay of remanent magnetization.[21] The remanent magnetization is related to the blocking function distribution by

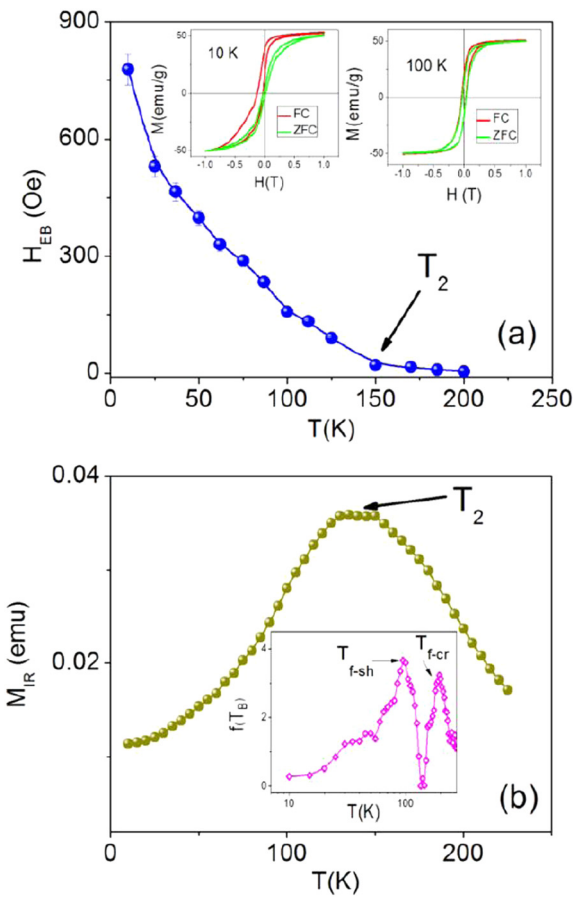

FIG. 3. (a) Temperature dependence of exchange bias field for cooling field of 1 T and (b) temperature dependence of isothermal remanence. Insets in (a) show the ZFC and FC hysteresis loops at 10 K and 100 K. Inset in (b) shows the temperature dependence of blocking function distribution.

$$I_r(T) = \alpha M_s \int_T^\infty f(T_B) dT_B. \quad (1)$$

The parameter α takes into account the random orientation of anisotropy in the nanoparticles,[22] and M_s is the saturation magnetization. The blocking temperature distribution function $f(T_B)$ can be estimated from the derivative of Eq. (1), i.e., $\frac{dI_r}{dT} \propto f(T_B)$. The temperature dependence of isothermal remanent magnetization (M_{IR}) is shown in Fig. 3(b). As the temperature decreases, M_{IR} increases steadily and reaches a maximum ~160 K below which it decreases. Such a behavior in M_{IR} is rather unconventional but has also been reported in the case of core-shell Fe/γ-Fe_2O_3 nanoparticles. The drop in M_{IR} below 160 K can be attributed to the blocking of the individual grains constituting the shell in random directions, as a result of which the effective magnetization (at zero field) per nanoparticle drops.[6] It is reasonable to claim that the blocking of the shell moments at 160 K enhances the anisotropy of the AFM shell, thus aiding the pinning of FM core moments as it is reversed. This leads to a distinct rise in H_{EB} from $T_2 \sim 160$ K [Fig. 3(a)]. In the inset of Fig. 3(b), the temperature dependence of the blocking function distribution shows two prominent peaks at ~190 K and ~95 K. The peak in the energy barrier distribution at 190 K occurs above the blocking temperature of the shell moments ($T_2 \sim 160$ K). Since the shell moments are superparamagnetic at $T > T_2$, the contribution to the energy barrier is solely from the core moments at 190 K. So, as the temperature is lowered from room temperature to 190 K, the core moments undergo a crossover from an individual blocked state to a collective frozen state, which is associated with a maximum in the energy barrier distribution ($T_{f\text{-}cr} \sim 190$ K). Below the freezing temperature of the core, the nanoparticles begin to exhibit EB. It was shown experimentally that the onset of EB is marked by the temperature where the core moments are frozen and the shell begins to show blocking behavior.[6] Although, the blocking temperature of the shell moments is $T_2 \sim 160$ K, the possibility of some blocked shell moments at 190 K cannot be ruled out due to the presence of finite size distribution in the nanoparticles. This explains why EB is seen albeit not substantially pronounced between 190 K and 160 K. It is only below the blocking temperature of the shell moments (T_2) that EB is enhanced as discussed earlier. The second peak in the energy barrier distribution at ~95 K occurs below the freezing temperature of the core and the blocking temperature of the shell. We attribute this peak to the freezing of the shell moments ($T_{f\text{-}sh}$) which is consistent with earlier reports.[6] Interestingly, the FC hysteresis loops measured below $T_{f\text{-}sh}$ become asymmetric and the degree of asymmetry increases as the measurement temperature is further lowered. This is evident from the insets of Fig. 3(a) where the FC loop is symmetric at 100 K, but highly asymmetric at 10 K. Thus, from the above analyses, we have identified three characteristic temperatures below T_N; (i) the freezing temperature of FM core moments at $T_{f\text{-}cr} \sim 190$ K which marks the onset of EB, (ii) the blocking temperature of the AFM shell moments at $T_2 \sim 160$ K leading to enhancement of EB, and (iii) freezing temperature of the AFM shell moments at $T_1 \sim T_{f\text{-}sh} \sim 95$ K below which asymmetry in the FC hysteresis loops is observed.

In earlier reports, the presence of asymmetric FC hysteresis loops has been attributed to competing anisotropy,[16] increase in interface coupling.[12] In case of FM/AFM bilayers, the angle between the easy axis and magnetic field direction is responsible for the asymmetry.[16] The development of asymmetry in the FC hysteresis loop suggests the role of different reversal mechanisms in the demagnetizing and return curves influenced by the magnetic anisotropy. It has been studied that the presence of small clusters of Co in the diffusion layer around the Co core may be responsible for asymmetry.[4] However, such clusters which appear as defect sites in the CoO shell exhibit a low temperature paramagnetic response associated with a sharp rise in magnetization. In the case of our sample, no such low temperature paramagnetic response was observed, which rules out the presence of any defect in CoO that could be responsible for the observed asymmetry. This implies that the asymmetry in FC hysteresis loops below $T_{f\text{-}sh}$ is an intrinsic property and that its development is controlled by the local anisotropy of the core and shell.

To understand the evolution of effective magnetic anisotropy field with temperature and its relationship to EB, radio frequency transverse susceptibility measurements based on a tunnel diode oscillator (TDO) were conducted. In this technique, a self-resonating LC tank circuit generates a small rf (f ~ 12 MHz) magnetic field (<10 Oe) that is applied transverse to the variable external dc field. The sample is placed in an inductive coil, which is a part of the resonating circuit. As the dc magnetic field or temperature is varied, the inductance of the coil changes which in turn shifts the resonant frequency by Δf. The relative change in the resonance frequency gives a direct measure of the change in transverse susceptibility ($\Delta\chi_T$) as shown in Eq. (2).

$$\frac{\Delta f}{f} \propto \left(\frac{\Delta\chi_T}{\chi_T}\right)\% = \frac{[\chi_T(H) - \chi_T^{sat}] \times 100}{\chi_T^{sat}}. \quad (2)$$

Here, $\chi_T(H)$ and χ_T^{sat} are TS values at magnetic field H and saturation, respectively. This technique is excellent to probe subtle dynamic magnetic responses associated with change in magnetic anisotropy.[23–27] More details on the experimental set up can be found elsewhere.[28] A typical experimental procedure is to cool the sample in the absence (ZFC-TS)/presence (FC-TS) of a magnetic field to a fixed temperature and then sweep the magnetic field from positive saturation to negative saturation (unipolar scan) and back to positive saturation for a bipolar scan.

Unipolar ZFC-TS curves in the temperature range of 10 K to 300 K and within the magnetic field range ± 1 T are shown in Fig. 4(a). In a unipolar scan, as the magnetic field is swept from positive to negative saturation at a constant temperature, two distinct peaks develop [Fig. 4(b)] that correspond to the first (H_{K1}) and second ($-H_{K2}$) anisotropy fields, which is consistent with the theoretical prediction by Aharoni *et al.* and other experimental results.[24,25,29] The temperature dependence of the anisotropy fields is shown in Fig. 4(c). The magnitude of anisotropy fields (H_{K1} and $-H_{K2}$) increases as the temperature is lowered down to T_2 below which a nominal decrease is noticed. On further cooling, a sharp rise is observed at $T_{f\text{-}sh}$. While the sample is cooled from room temperature, the primary contribution to the anisotropy is from the core; however, as the temperature crosses T_2, the blocking of the shell moments in

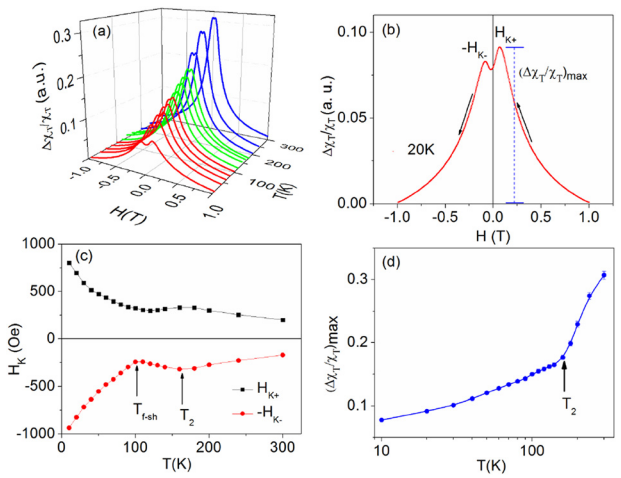

FIG. 4. (a) 3D plot of unipolar TS scans showing temperature and magnetic field dependence under ZFC conditions, (b) representative unipolar TS scan at 20 K to illustrate the peaks at anisotropy field and the maximum value of $\frac{\Delta\chi_T}{\chi_T}$, (c) temperature dependence of effective anisotropy fields, (d) temperature dependence of $\left(\frac{\Delta\chi_T}{\chi_T}\right)_{max}$.

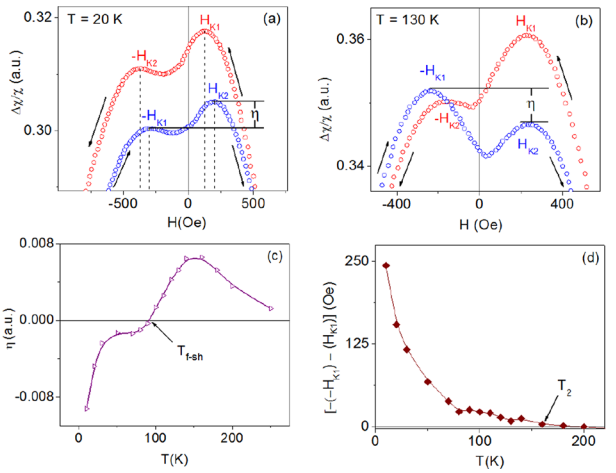

FIG. 5. (a) and (b) Bipolar TS scan at 20 K and 130 K under FC condition indicating the anisotropy fields and η, (c) temperature dependence of η, (d) temperature dependence of shift in the first anisotropy peaks in the bipolar scans.

random direction nominally reduces the effective anisotropy field as seen in Fig. 4(c). The freezing of the shell moments at $T_{f\text{-}sh}$ introduces additional anisotropy which can be seen as the sharp rise in $-H_{K2}$ that increases progressively as the temperature is lowered. The maximum change in TS $[(\Delta\chi/\chi)_{max}]$ is sensitive to any change in the dynamic magnetic state.[24] In Fig. 4(d), the temperature dependence of $(\Delta\chi/\chi)_{max}$ shows a gradual increase up to $T_2 \sim 160$ K followed by a rapid increase in TS peak height which marks the unblocking of shell moments and simultaneous suppression of EB in the system. At room temperature, the presence of anisotropy peaks [Fig. 4(c)] corroborates the fact that the core is still in the blocked state. We expect the two anisotropy peaks to merge into a single peak at the blocking temperature of the core moments above which the nanoparticles will be completely superparamagnetic.[25]

The effect of field cooling on the magnetic anisotropy is pivotal in understanding the mechanism responsible for such asymmetric loops. We performed FC-TS measurements in the temperature range of 10 K to 300 K by cooling under an applied field of 1 T. Figures 5(a) and 5(b) show the TS curves for bipolar scans at 20 K and 130 K which represent temperatures below and above $T_{f\text{-}sh}$, respectively. In both cases [Figs. 5(a) and 5(b)], while the dc magnetic field is swept from positive to negative saturation, the first (H_{K1}) peak is higher than the second $(-H_{K2})$ peak. This is qualitatively understood from the perspective of competition between the Zeeman energy (which dominates near saturation and causes forcible alignment of moments in field direction while cooling) and anisotropy energy (which dominates near zero field).[26] Similarly, when the field is swept from negative to positive saturation in the return curve, one would expect the first $(-H_{K1})$ peak to be higher than the second (H_{K2}) peak. This is seen in the TS curves at 130 K [Fig. 5(b)], but, at 20 K [Fig 5(a)], the first $(-H_{K1})$ peak is lower than the second (H_{K2}) peak contrary to previous results.[25,26] We plotted [Fig. 5(c)] the difference in peak height (η) with respect to temperature for the return TS curve. Negative values of η indicate that the peak height of $-H_{K1}$ is lower than H_{K2}. As the temperature is decreased, the value of η crosses over from positive to negative at $T_{f\text{-}sh} \sim 95$ K. This can be understood as follows; the freezing of shell moments along the cooling field direction introduces additional anisotropy energy which dominates over the Zeeman energy in the return curve. This additional anisotropy energy persists up to $T_{f\text{-}sh}$ and vanishes for higher temperatures yielding conventional FC-TS return curves and symmetric FC hysteresis loops (inset of Fig. 3(a)). The temperature dependence of the relative shift of the first anisotropy field $[-(-H_{K1}) - (H_{K1})]$ is shown in Fig. 5(b). The nature of the curve shows striking resemblance to $H_{EB}(T)$ curve [Fig. 3(a)]. The shift in anisotropy field decreases as the temperature is increased, and becomes highly diminished above T_2 as indicated.

In summary, we have studied the static and dynamic magnetic properties of Co/CoO core-shell nanoparticles. We are able to map out the temperature dependent energy barrier distribution which allows us to identify $T_{f\text{-}cr}$ (freezing of core moments triggering onset of EB), T_2 (blocking temperature of shell moments), and $T_{f\text{-}sh}$ (freezing temperature of shell moments). The field cooled hysteresis loops exhibit exchange bias and are found to be symmetric and asymmetric above and below freezing temperature of the shell moments, respectively. The TS measurements are highly consistent with our above findings thus proving to be an excellent probe for low temperature magnetic phenomena. We have shown clear evidence of shell freezing due to which the anisotropy energy overcomes the Zeeman energy below $T_{f\text{-}sh}$ resulting in asymmetric hysteresis. The temperature dependence of shift in anisotropy field on field cooling follows a similar trend as EB field and vanishes above $T_{f\text{-}cr}$. Hence, from our result we conclude that the magnetic anisotropy associated with the "shell" controls the nature of the FC hysteresis loops for materials exhibiting EB and an appropriate selection of the "shell" material with known freezing temperature, will allow us to tune onset of asymmetry in the temperature scale.

The research was supported by DOE through Grant No. DE-FG02-07ER46438. H.S. also acknowledges the support from the Center for Integrated Functional Materials through Grant No. USAMRMC W81XWH-10-2-0101. M.H.P. thanks the support from Florida Cluster for Advanced Smart Sensor Technologies.

[1]R. L. Stamps, J. Phys. D: Appl. Phys. **33**(23), R247 (2000).
[2]M. Kiwi, J. Magn. Magn. Mater. **234**(3), 584 (2001).
[3]J. Nogues and I. K. Schuller, J. Magn. Magn. Mater. **192**(2), 203 (1999).
[4]J. B. Tracy, D. N. Weiss, D. P. Dinega, and M. G. Bawendi, Phys. Rev. B **72**(6), 064404 (2005).
[5]M. Feygenson, Y. Yiu, A. Kou, K.-S. Kim, and M. C. Aronson, Phys. Rev. B **81**(19), 195445 (2010).
[6]S. Chandra, H. Khurshid, W. Li, G. C. Hadjipanayis, M. H. Phan, and H. Srikanth, Phys. Rev. B **86**, 014426 (2012).
[7]X. Sun, N. F. Huls, A. Sigdel, and S. Sun, Nano Lett. **12**(1), 246 (2012).
[8]Q. K. Ong, A. Wei, and X.-M. Lin, Phys. Rev. B **80**(13), 134418 (2009).
[9]H. Khurshid, W. Li, M.-H. Phan, P. Mukherjee, G. C. Hadjipanayis, and H. Srikanth, Appl. Phys. Lett. **101**, 022403 (2012).
[10]Y. Hu, Y. Liu, and A. Du, J. Appl. Phys. **108**(3), 033904 (2010).
[11]A. N. Dobrynin, D. N. Ievlev, K. Temst, P. Lievens, J. Margueritat, J. Gonzalo, C. N. Afonso, S. Q. Zhou, A. Vantomme, E. Piscopiello, and G. Van Tendeloo, Appl. Phys. Lett. **87**(1), 012501 (2005).
[12]O. Iglesias, X. Batlle, and A. Labarta, Phys. Rev. B **72**(21), 212401 (2005).
[13]O. Iglesias, X. Batlle, and A. Labarta, J. Magn. Magn. Mater. **316**(2), 140 (2007).
[14]A. Cabot, A. Paul Alivisatos, V. F. Puntes, L. Balcells, O. Iglesias, and A. Labarta, Phys. Rev. B **79**(9), 094419 (2009).
[15]D. L. Peng, T. Hihara, K. Sumiyama, and H. Morikawa, J. Appl. Phys. **92**(6), 3075 (2002).
[16]J. Camarero, J. Sort, A. Hoffmann, J. M. Garcia-Martin, B. Dieny, R. Miranda, and J. Nogues, Phys. Rev. Lett. **95**(5), 057204 (2005).
[17]J. Nogues, V. Skumryev, J. Sort, S. Stoyanov, and D. Givord, Phys. Rev. Lett. **97**(15), 157203 (2006).
[18]H. T. Yang, C. M. Shen, Y. G. Wang, Y. K. Su, T. Z. Yang, and H. J. Gao, Nanotechnology **15**(1), 70 (2004).
[19]G. Hassnain Jaffari, S. Rizwan Ali, S. K. Hasanain, G. Guentherodt, and S. Ismat Shah, J. Appl. Phys. **108**(6), 063921 (2010).
[20]S. Gangopadhyay, G. C. Hadjipanayis, C. M. Sorensen, and K. J. Klabunde, J. Appl. Phys. **73**(10), 6964 (1993).
[21]R. W. Chantrell, M. Elhilo, and K. Ogrady, IEEE Trans. Magn. **27**(4), 3570 (1991).
[22]C. P. Bean, J. D. Livingston, and D. S. Rodbell, J. Phys. Radium **20**(2–3), 298 (1959).
[23]S. Chandra, A. I. Figueroa, B. Ghosh, A. K. Raychaudhuri, M. H. Phan, P. Mukherjee, and H. Srikanth, Physica B **407**(1), 175 (2012).
[24]S. Chandra, A. I. Figueroa, B. Ghosh, M. H. Phan, H. Srikanth, and A. K. Raychaudhuri, J. Appl. Phys. **109**(7), 07D720 (2011).
[25]P. Poddar, J. L. Wilson, H. Srikanth, D. F. Farrell, and S. A. Majetich, Phys. Rev. B **68**(21), 214409 (2003).
[26]P. Poddar, M. B. Morales, N. A. Frey, S. A. Morrison, E. E. Carpenter, and H. Srikanth, J. Appl. Phys. **104**(6), 063901 (2008).
[27]N. A. Frey Huls, N. S. Bingham, M. H. Phan, H. Srikanth, D. D. Stauffer, and C. Leighton, Phys. Rev. B **83**(2), 024406 (2011).
[28]H. Srikanth, J. Wiggins, and H. Rees, Rev. Sci. Instrum. **70**(7), 3097 (1999).
[29]A. Aharoni, E. H. Frei, S. Shtrikman, and D. Treves, Bull. Res. Counc. Isr., Sect. F **6A**, 215 (1957).